UNIVERSIDAD NACIONAL DE COLOMBIA
SEDE MEDELLÍN
FACULTAD DE MINAS

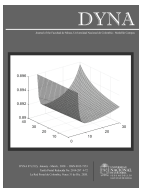

DYNA
http://dyna.medellin.unal.edu.co/

Prediction of *in vitro* release of nanoencapsulated phenolic compounds using Artificial Neural Networks

Luz América Espinosa-Sandoval, Claudia Isabel Ochoa-Martínez & Alfredo Adolfo Ayala-Aponte

Facultad de Ingeniería, Escuela de Ingeniería de Alimentos, Universidad del Valle, Colombia. luz.a.espinosa@correounivalle.edu.co, claudia.ochoa@correounivalle.edu.co, alfredo.ayala@correounivalle.edu.co

Received: June 15th, de 2018. Received in revised form: April 24th, 2019. Accepted: June 16th, 2019

Abstract
In Vitro Release modeling (IVR) of nanoencapsulated phenolic compounds (PC) is complex, due to the number of factors involved in the process. Artificial Neural Networks (ANN) are useful tools for its prediction because they consider the effect of all factors on the response. The release at 5h is crucial in kinetics because, in most cases, it is an equilibrium point leading to a constant phase. The objective of this investigation was to predict the IVR of nanoencapsulated PC at 5h using ANN. A database with information from the scientific literature was used. This model permits mathematical correlation of the IVR at 5h with eleven factors. The optimal network configuration consisted of one hidden layer with one neuron. A mathematical model was obtained with a Mean Square Error (MSE) of 0.0516 and a correlation coefficient (*r*) of 0.8413.

Keywords: : phenolic compounds; ultrasound; nanoencapsulation; Artificial Neural Networks (ANN).

Predicción de la liberación *in vitro* de compuestos fenólicos nanoencapsulados empleando Redes Neuronales Artificiales

Resumen
La modelación de la liberación in vitro (LIV) de compuestos fenólicos (CF) nanoencapsulados es compleja debido a la cantidad de factores que intervienen en el proceso. Las Redes Neuronales Artificiales (RNA) constituyen una herramienta útil para predecirla gracias a que consideran el efecto de todos los factores sobre la respuesta. La LIV a 5h es determinante en las cinéticas debido a que en la mayoría de las investigaciones se alcanza un punto de equilibrio y se pasa a una fase constante. El objetivo de esta investigación fue predecir la LIV a 5h de CF nanoencapsulados empleando RNA. El modelo desarrollado permite correlacionar matemáticamente la LIV a 5h de CF nanoencapsulados con once factores. La configuración óptima de la red consistió de una capa oculta con una neurona. Se obtuvo un modelo matemático con un Error Cuadrático Medio (ECM) de 0.0516 y un coeficiente de correlación (*r)* de 0.8413.

Palabras clave: compuestos fenólicos; ultrasonido; nanoencapsulación; Redes Neuronales Artificiales (ANN).

1. Introduction

Phenolic compounds (PC) are molecular agents present in foods that exhibit the ability to modulate one or more metabolic processes. They generate special interest in the scientific community, owing to their health benefits, which has been demonstrated in studies that address their effects and risk-prevention actions for certain diseases [1].

One of the biggest challenges barring the development of food enriched with PC, called functional food, is to find ways to integrate these into food matrices without negatively affecting the psychosensory properties of the final product [2]. To solve this problem, the field of nanotechnology has enabled the design of PC supply systems on a nanoscale (20-1000 nm) from PC nanoencapsulation by means of nanoemulsions applying ultrasound. This process offers multiple advantages, such as the possibility of transporting PC through the bloodstream and controlling their release to specific organs or tissues in the required doses [3].

How to cite: Espinosa-Sandoval, L.A, Ochoa-Martínez, C.I. and Ayala-Aponte, A.A, Prediction of in vitro release of nanoencapsulated phenolic compounds using Artificial Neural Networks. DYNA, 87(212), pp. 244-250, January - March, 2020.

The modeling of the process is complex due to the number of factors and the transfer phenomena (heat and mass) that are involved. Thus, Artificial Neural Networks (ANN) are useful tools for the development of mathematical models, thanks to the wide range of factors that are considered for model formulation and their straightforward implementation [4].

Various authors have used ANN methodology to predict response variables in food processes; for example, in osmotic dehydration [5], extrusion [6], drying [7], milling [8], sensory analysis [9], fermentation [10], among others. However, the IVR prediction of nanoencapsulated active compounds has been studied mainly in the pharmaceuticals and cosmetics fields [11-14], but not in the development of functional foods.

IVR at 5h is determinant in kinetics because, in most studies, the release of the PC reaches an equilibrium point going from an increase to a permanent stage until total PC is brought out. The objective of this investigation was to predict IVR at 5h following PC nanoencapsulation, using a mathematical correlation model via ANN.

2. Materials and methods

2.1. Database preparation

A database with information obtained from the scientific literature was built. A total of 52 pieces of data from 15 scientific articles [15-29] was used. Several items were discarded because they did not include all of the information required for database creation. The data obtained were grouped randomly into three groups: a training group (corresponding to 65% of the data), a cross-validation group (15%), and a verification group (20%). Microsoft Excel Software was used to store the data. The process factors included PC mass, concentration, polymeric relationship (referring to the relationship that exists between encapsulating polymers when used from one to three polymers to carry out the PC encapsulation, the sum of the three must always be 1) totally encapsulating copolymer mass, solvent volume, surfactant concentration, emulsion volume, time, and ultrasound power. The response variable was the in vitro release five hours following PC nanoencapsulation. In vitro PC release is calculated using EQ. (1):

$$IVR = \left(\frac{m_t}{m_\infty}\right)(100) \tag{1}$$

Where, m_t is the concentration of PC at five hours, and m_∞ is the concentration of the PC at $t = \infty$.

2.2. Multivariate regression

Prior to the use of the ANN methodology, a multivariate analysis was carried out using the Microsoft Excel Software's linear correlation tool.

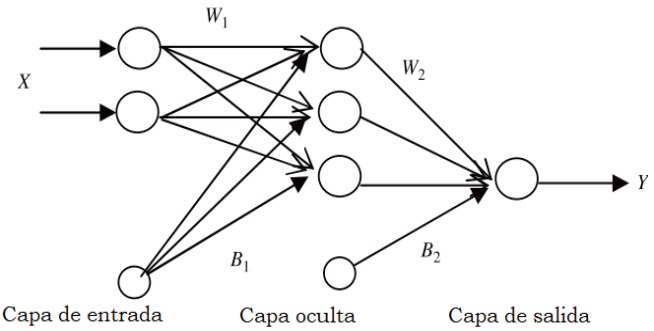

Figure 1. General ANN outline
Adapted from [33].

2.3. Architecture of ANN

In Fig. 1, the general ANN outline is presented, where the *Xs* are the independent variables, w_1 and B_1 are the weights and bias for the hidden layer, and w_2 and B_2 are the weights and bias for the output layer. Finally, and *Y* is the answer.

Table 1 shows the ANN architecture used for training. The number of neurons in the input layer is 11 (nine independent variables) because the x_2, x_3, and x_4 factors correspond to a single independent variable, and are dependent upon each other. For the development of the model, the Mean Square Error (MSE), defined by Eq. (2) and the correlation coefficient (*r*) were used as the termination criteria.

$$MSE = \sum_{i=1}^{N} \frac{\left(K_p - K_d\right)^2}{N} \tag{2}$$

Where k_p and k_d are the predicted and experimental values, respectively, and *N* is the total number of data.

The activation function computes the activity status of a neuron by calculating the global input at an activation value [30]. The most common functions are the sigmoidal logistic function, Eq. (3), and the hyperbolic tangent function, Eq. (4).

$$f(x) = \frac{1}{1 + e^{-x}} \tag{3}$$

Table 1.
ANN Architecture

Caracteristic	Configuration
Network type	Multi-layer perceptron
Number of input neurons	11 (factors)
Number of output neurons	1 (response variable)
Number of hidden layers	1
Number of neurons in the hidden layer	1-7
Transfer function for the hidden layer	Sigmoidal logistics, tanh
Transfer function for the output layer	Linear
Learning rule	Modified Delta Rule
Step size for the hidden layer	1.0
Step size for the output layer	0.1
Momentum constant	0.7
Termination criteria	MSE
Number of maximum epochs	1000

Source: The Authors.

$$\tanh(x) = \frac{e^{x} - e^{-x}}{e^{x} + e^{-x}} \quad (4)$$

In order to improve the behavior of the ANN, the input and output values of the network were standardized using Eq. (5) [31].

$$data\ norm_{(i)} = \left(amplitude_{(i)}\right)\left(data_{(i)}\right) + offset_{(i)} \quad (5)$$

Where *data norm(i)* refers to the standardized data for each *i* variable, *data(i)* is the data entered by the user for each *i,* and *amplitude(i)* and $offset_{(i)}$ (compensation) are coefficients calculated for each *i* by eqs. 6, 7.

$$amplitude_{(i)} = \frac{upper\ bound\ -\ lower\ bound}{Max_{(i)} - Min_{(i)}} \quad (6)$$

$$offset_{(i)} = upper\ bound - (amplitude_{(i)})(Max_{(i)}) \quad (7)$$

The upper and lower values are the limits of the normalized value, and $Max_{(i)}$ and $Min_{(i)}$ are the maximum and minimum values found within variable *i*.

2.4. Training and cross-validation

For network training, the commercial software, NeuroSolutions 2016, was employed. The training was performed within the architecture defined in Table 1, varying the number of neurons in the hidden layer and the transfer function. The training process was repeated several times, in order to obtain the lowest MSE. Successful training was achieved when the curve between learning and cross-validation (MSE vs. Epoch) approached zero [32]. Verification was developed with the best weights, stored during training and cross-validation.

2.5. Model

The model is expressed by the matrix in Eq. (8).

$$Y = f_2(W_2 f_1(W_1 X + B_1) + B_2) \quad (8)$$

Where ***Y*** is the array of output variables, f_1 and f_2 are the activation functions in the hidden and output layers, respectively, and ***X*** is the input variable array [33].

2.6. ANN performance

ANN performed with through experimental verification values. The MSE, the mean absolute error (MAE) Eq. 9, the Mean Relative Error (MRE) Eq. 10 and the correlation coefficient *(r)* were used as criteria.

$$EAM = |X_{iobs} - X_i| \quad (9)$$

$$ERM = \frac{|X_{iobs} - X_i|}{x_{iobs}} \quad (10)$$

Where, x_{iobs} is the experimental value for *i,* and x_i is the value predicted by the model.

2.7. Sensitivity analysis

The sensitivity analysis was developed in accordance with the methodology established by [33]. This analysis was carried out in order to evaluate the effect of each input variable on the response variable. For this, noise was incorporated into each input variable, using a Gaussian error of 5% (σ = 5%) with a 98% probability (the standard adding or resetting value is 2.576σ at each input value, taking into account a Box Behnken composite central design (Table 2) with 289 combinations for 11 factors. The entire database (52 data) was assessed, for a total of 165,308 cases.

Table 2.
Box-Behnken composite central design for the sensitivity analysis

Group run	x_1	x_2	x_3	x_4	x_5	x_6	x_7	x_8	x_9	x_{10}	x_{11}
1	0	0	0	0	0	0	0	0	0	0	0
2	1	1	1	1	1	1	1	1	1	1	1
3	-1	-1	-1	-1	-1	-1	-1	-1	-1	-1	-1
4	0	0	±1	0	0	0	±1	±1	±1	0	±1
5	±1	0	0	±1	0	0	0	±1	±1	±1	0
6	0	±1	0	0	±1	0	0	0	±1	±1	±1
7	±1	0	±1	0	0	±1	0	0	0	±1	±1
8	±1	±1	0	±1	0	0	±1	0	0	0	±1
9	±1	±1	±1	0	±1	0	0	±1	0	0	0
10	0	±1	±1	±1	0	±1	0	0	±1	0	0
11	0	0	±1	±1	±1	0	±1	0	0	±1	0
12	0	0	0	±1	±1	±1	0	±1	0	0	±1
13	±1	0	0	0	±1	±1	±1	0	±1	0	0
14	0	±1	0	0	0	±1	±1	±1	0	±1	0

x_1 is the bioactive compound mass (mg); x_2, x_3, and x_4 is the encapsulating polymeric relationship (e.g. Poly (DL-lactide-co-glycolide) PLGA is a copolymer with two polymers. In this case, the relationship between the copolymer is placed in the variables and if there is no third polymer is placed zero, thus, a 50:50 PLGA would be $x_2 = 50$, $x_3 = 50$, and $x_4 = 0$), x_5 polymer concentration (mg/mL water); x_6 polymer mass (mg); x_7 solvent volume (mL); x_8 surfactant concentration (mg/mL water); x_9 emulsion volume (mL); x_{10} ultrasound time (min) and x_{11} ultrasound power (W)
Source: The Authors.

Table 3.
Valid range of factors and response variables

Factor and response variable	Minimum	Maximum
PC mass (mg)	2	20
Polymer 1	0	100
Polymer 2	0	100
Polymer 3	0	100
Polymer concentration (mg/mL water)	1	20
Polymer mass (mg)	0.5	200
Solvent volume (mL)	0.5	27
Surfactant concentration (mg/mL water)	0.1	2
Emulsion volume (mL)	10	150
Ultrasound time (min)	0.5	30
Ultrasound power (W)	50	750
Five-hour IVR (mg PC/ total mg PC)	0	1

Source: The Authors.

Finally, the MSE was calculated between the base case (no noise) and the combination of response variables defined in accordance with the design. The average of all MSE's in each run group (Table 2) was plotted.

2.8. Simulation and optimization

Optimal conditions depend on the final use of the nanoparticle. In this study, the five-hour IVR was maximized. A mixture design with eight factors was used, taking into account the ranges established for each factor (Table 3). R Statistical Software was used.

3. Results and discussion

3.1. Multivariate analysis

The polynomial regression allowed to analyze 7 independent variables for the IVR at 5h and a MSE of 606 (*r* of 0.17) was obtained. Through this analysis, it could be confirmed that it is not possible to develop a polynomial regression model to correlate mathematically all the factors with the response variable. In addition, the MSE presents very high values and the correlation coefficient is not adjusted. This implies that another methodology is required to obtain a correlation to predict the IVR at 5h. The methodology of ANN has been useful in cases of high complexity because they consider the effect of all the factors on the answer [11].

3.2. Process elements and transfer function in the hidden layer

Table 4 shows the effect of the number of neurons and the transfer function in the hidden layer over the difference between the desired output and that obtained with the model by means of the MSE and *r*.

The optimal ANN consisted of a hidden layer with one neuron. The transfer function that allowed to predict the response was Sigmoidal Logistics (eq. (5)). The model presented a MSE of 0.0516 and an *r* of 0.8413. When performing an analysis of variance, it was noted that the model allows to predict the IVR at 5h of nanoencapsulated PC with a statistically significant generalization ($p < 0.05$) within the ranges established for the model.

Table 4.
Effect of the number of neurons and the transfer function over the MSE and r for the IVR at 5h

Neurons number	IVR at 5h			
	Tanh		Sig log	
	MSE	*r*	MSE	*r*
1	0.2263	0.6615	**0.0516**	**0.8413**
2	0.1725	0.5334	0.2115	0.6748
3	0.3113	0.3524	0.2333	0.5624
4	0.2665	0.5541	0.2254	0.3455
5	0.2678	0.3218	0.2267	0.2816
6	0.2659	0.3675	0.2285	0.2345
7	0.2664	0.2546	0.2291	0.3112

Source: The Authors.

3.3. Model

The mathematical correlation between the factors and the IVR to 5h can be represented by the algebraic system eqs. (11, 12).

$$IVR_{5h} = \left(\frac{1.78}{1+e^{-y_1}} + 0.105\right)/2.142 \tag{11}$$

$$y_1 = 5.91\times10^{-2}x_1 + 9.77\times10^{-3}x_2 + 1.11\times10^{-2}x_3 - 8.61\times10^{-2}x_4 + 4.23\times10^{-2}x_5 + 1.07\times10^{-2}x_6 + 1.19\times10^{-3}x_7 - 2.30x_8 - 1.51\times10^{-2}x_9 - 1.39\times10^{-2}x_{10} + 1.86\times10^{-3}x_{11} - 0.839 \tag{12}$$

Where, x_1 is the quantity of PC (mg); x_2, x_3 and x_4 is the relationship between encapsulating polymers, x_5 is the concentration of the polymer (mg/mL water), x_6 is the quantity of the polymer (mg); x_7 is the volume of solvent (mL); x_8 is the surfactant concentration (mg/mL water); x_9 emulsion volume (mL); x_{10} is the ultrasound time (min), and x_{11} is ultrasound power (W).

The algebraic equation system can be easily programmed into a spreadsheet in Microsoft Excel, so as to determine the nanoencapsulated PC IVR at five hours.

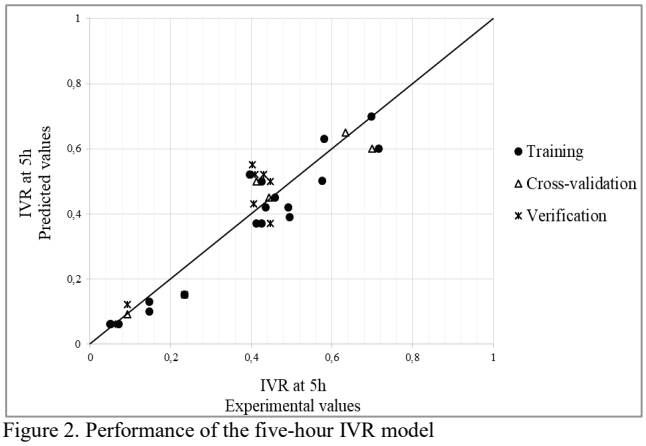

Figure 2. Performance of the five-hour IVR model
Source: The Authors.

3.4. ANN performance

In Fig. 2, the correlation between the values predicted by the model and the experimental values taken for training, cross-validation, and verification are shown. When the AN performance is evaluated with new data for verification, the predicted values approached experimental values, and the training MSE was corroborated. An *r* of 0.8413, a MAE of 0.1091, and an MRE of 0.1372 were obtained. These results show an approximation to a normal distribution near zero, with 95% probability. The model is capable of predicting, with statistically significant probability ($P < 0.05$), the IVR at five hours, when the model is processed with new data.

3.5. Sensitivity analysis

The model presents high sensitivity to surfactant concentration, since all points related to this factor showed an MSE of greater than 0.054 (Fig. 3). The other factors did not have an effect on the model's sensitivity to "noise". Phenomenologically, this is because the surfactant influences surface tension of the contact surface between the aqueous and the oily emulsion phase. Therefore, it is the one that permits emulsion maintenance, in order to create nanoparticles and release the compound at the required rate [34]. Another explanation for this sensitivity is given by authors including [35, 36] who have proven that there is a connection between principal component analysis and neural networks. These authors suggest that, when a multi-layered perceptron network that learns from a retropropagation algorithm and monitored by a self-associative mode is used to train a neural network, it is possible to obtain a self-organized system, with feed-forward synaptic connections from the factors to the response variables. The strength of network synaptic connections (synaptic weights) is modified in accordance with the response of the neural signal, due to synaptic plasticity in descending order.

Table 5 shows that, when performing a principal component analysis, the factor that presents the highest absolute weight value is the surfactant concentration, and therefore, this is the factor that presents greatest sensitivity to "noise". This is corroborated by the main effects graph in Fig. 4.

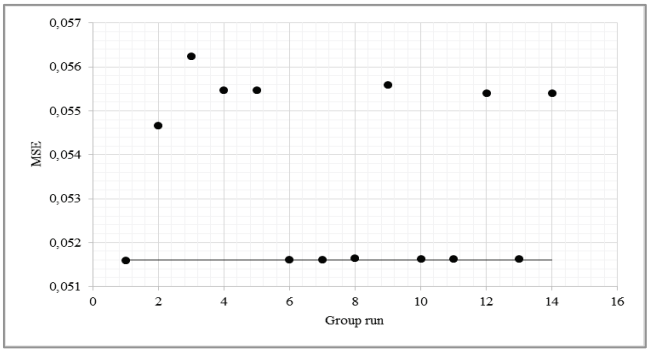

Figure 3. Sensitivity analysis for the five-hour IVR model. (-) basic case without "noise".
Source: The Authors.

Table 5.
Standard weights for five-hour IVR model

Factors	Synaptic weights
	w_1
PC mass (mg)	0.0591
Polymer 1	0.0098
Polymer 2	0.0111
Polymer 3	-0.0861
Polymer concentration (mg/mL water)	0.0423
Polymer mass (mg)	0.0107
Solvent volume (mL)	0.0012
Surfactant concentration (mg/mL water)	**-2.3041**
Emulsion volume (mL)	-0.0151
Ultrasound time (min)	-0.0139
Ultrasound power (W)	0.0019

Source: The Authors.

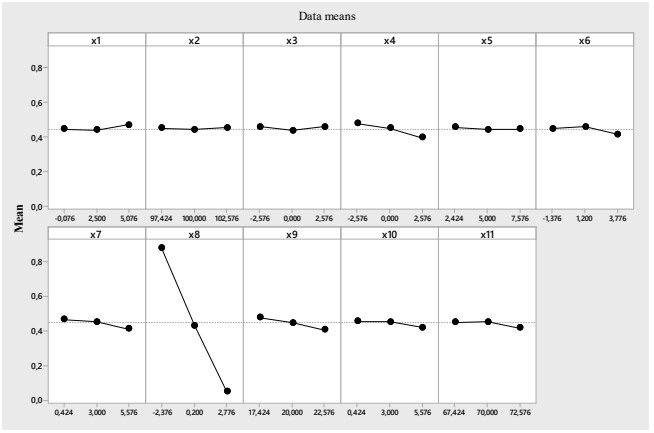

Figure 4. Main effects for five-hour IVR model
Source: The Authors.

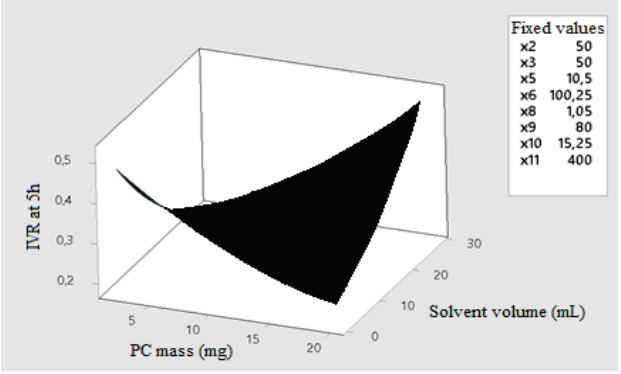

Figure 5. Effect of the relation between PC mass – solvent volume over the five-hour IVR
Source: The Authors.

3.6. Simulation

According to the Pareto diagram of standardized effects, factors that have statistically significant effects ($p < 0.05$) on five-hour IVR include the relation between the PC mass-solvent volume (Fig. 5), and relation between the surfactant concentration-emulsion volume (Fig. 6). Fig. 5 shows that, as the PC mass and solvent volume increases, the IVR also

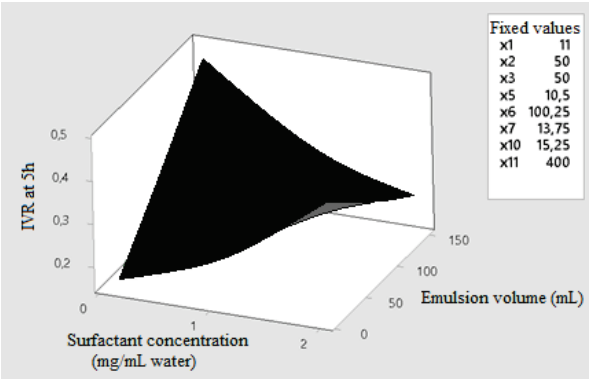

Figure 6. Effect of the relationship between surfactant concentration – emulsion volume over the five-hour IVR
Source: The Authors.

Table 6.
Five-hour IVR maximization

Factors	Optimum
PC mass (mg)	20
Polymer 1	50
Polymer 2	50
Polymer 3	0
Polymer concentration (mg/mL water)	14
Polymer mass (mg)	0.5
Solvent volume (mL)	27
Surfactant concentration (mg/mL water)	2
Emulsion volume (mL)	150
Ultrasound time (min)	0.5
Ultrasound power (W)	50
IVR at 5h (mg PC/ total mg PC)	**0.99**

Source: The Authors.

increases because the solvent allows the PC to be scattered throughout the emulsion evenly, which broadens the release. On the other hand, in Fig. 6, it is observed that, as the volume of the emulsion increases at a surfactant concentration between 0.1 and 0.5, the five-hour IVR increases. This is because the IVR depends on several factors at the molecular level, such as the desorption of PC linked to the nanoassembly, the mechanisms of diffusion and erosion of the PC through the nanoparticle, and the chemical composition of the nanoparticle wall.

3.7. Optimization

A multivariate optimization was performed. Table 6 shows the optimal conditions of the factors that maximize the five-hour IVR. A desirable 0.9996 was obtained. It was observed that it is possible to release a mass fraction of 0.99 of the phenolic compound at that time.

4. Conclusions

The model developed by ANN makes it possible to mathematically correlate the in vitro release five hours after nanoencapsulating phenolic compounds with the PC mass, the relation, concentration, and mass of the encapsulating copolymer, solvent volume, surfactant concentration, emulsion volume, and ultrasound time and power. This model allows for prediction of the response variable with a mean square error (MSE) of 0.0516 and a correlation coefficient (r) of 0.8413, with a statistically significant generalization ($P < 0.05$).

Acknowledgements

One of the authors thanks COLCIENCIAS-COLFUTURO for funding her PhD (Luz America Espinosa-Sandoval).

References

[1] Kim, M.J., Moon, Y., Tou, J.C., Mou, B. and Waterland, N.L., Nutritional value, bioactive compounds and health benefits of lettuce (Lactuca sativa L.). Journal of Food Composition and Analysis, 49, pp. 19-34, 2016. DOI: 10.1016/j.jfca.2016.03.004

[2] Bogue, J., Collins, O. and Troy, A.J., Chapter 2 - Market analysis and concept development of functional foods. In: Developing New Functional Food and Nutraceutical Products, 2017, pp. 29-45. DOI: 10.1016/B978-0-12-802780-6.00002-X

[3] Leong, T., Martin, G. and Ashokkumar, M., Ultrasonic encapsulation: a review. Ultrasonics Sonochemestry, 35, pp. 605-614, 2017. DOI: 10.1016/j.ultsonch.2016.03.017

[4] Jamshidi, M., Ghaedi, M., Dashtian, K., Ghaedi, A.M., Hajati, S., Goudarzi, A. and Alipanahpour, E., Highly efficient simultaneous ultrasonic assisted adsorption of brilliant green and eosin B onto ZnS nanoparticles loaded activated carbon: Artificial neural network modeling and central composite design optimization. Spectrochimica Acta. Part A, Molecular and Biomolecular Spectroscopy, 153, pp. 257-267, 2015. DOI: 10.1016/j.saa.2015.08.024

[5] Ochoa-Martínes, C.I., Red neuronal artificial en respuesta a predicciones de parámetros de transferencia de masa (pérdida de humedad y ganancia de sólidos) durante la deshidratación osmótica de frutas. Acta Agronómica, 65(4), pp. 318-325, 2016.

[6] Cubeddu, A., Rauh, C. and Delgado, A., Hybrid artificial neural network for prediction and control of process variables in food extrusion. Innovative Food Science & Emerging Technologies, 21, pp. 142-150, 2014. DOI: 10.1016/j.ifset.2013.10.010

[7] Aktaş, M., Şevik, S., Özdemir, M.B. and Gönen, E., Performance analysis and modeling of a closed-loop heat pump dryer for bay leaves using artificial neural network. Applied Thermal Engineering, 87, pp. 714-723, 2015. DOI: 10.1016/j.applthermaleng.2015.05.049

[8] Sudha, L., Dillibabu, R., Srivatsa-Srinivas, S. and Annamalai, A., Optimization of process parameters in feed manufacturing using artificial neural network. Computers and Electronics in Agriculture, 120, pp. 1-6, 2016. DOI: 10.1016/j.compag.2015.11.004

[9] Górska-Horczyczak, E., Horczyczak, M., Guzek, D., Wojtasik-Kalinowska, I. and Wierzbicka, A., Chromatographic fingerprints supported by artificial neural network for differentiation of fresh and frozen pork. Food Control, 73, pp. 1-8, 2017. DOI: 10.1016/j.foodcont.2016.08.010

[10] Zeng, Z., Guo, X., Zhu, K., Peng, W., Zhou, H., Artifitial neural network. Genetic algorithm to optimize wheat germ fermentation condition: application to the production of two anti-tumor benzoquinones. Food Chemestry 227, pp. 264-270, 2017. DOI: 10.1016/j.foodchem.2017.01.077

[11] Sulaiman, I.S., Basri, M., Fard-Masoumi, H.R., Ashari, S.E., Basri, H. and Ismail, M., Predicting the optimum compositions of a transdermal nanoemulsion system containing an extract of *Clinacanthus nutans* leaves (L.) for skin antiaging by artificial neural network model. Journal of Chemometrics, e2894, pp. 1-13, 2017. DOI: 10.1002/cem.2894

[12] Tao, Y., Wang, P., Wang, J., Wu, Y., Han, Y. and Zhou, J., Combining various wall materials for encapsulation of blueberry anthocyanin extracts: Optimization by artificial neural network and genetic algorithm and a comprehensive analysis of anthocyanin powder properties. Powder Technology, 311, pp. 77-87, 2017. DOI:

10.1016/j.powtec.2017.01.078
[13] Shahsavari, S., Rezaie-Shirmard, L., Amini, M. and Abedin-Dokoosh, F., Application of artificial neural networks in the design and optimization of a nanoparticulate fingolimod delivery system based on biodegradable Poly(3-Hydroxybutyrate-Co-3-Hydroxyvalerate). Journal of Pharmaceutical Sciences, 106(1), pp. 176-182, 2017. DOI: 10.1016/j.xphs.2016.07.026
[14] Elkomy, M.H., Elmenshawe, S.F., Eid, H.M. and Ali, A.M.A., Topical ketoprofen nanogel: artificial neural network optimization, clustered bootstrap validation, and in vivo activity evaluation based on longitudinal dose response modeling. Drug Delivery, 7544, pp. 1-13, 2016. DOI: 10.1080/10717544.2016.1176086
[15] Pereira, M.C., Oliveira, D.A., Hill, L.E., Carlos, R., Borges, C.D., Vizzotto, M. and Gomes, C.L., Effect of nanoencapsulation using PLGA on antioxidant and antimicrobial activities of guabiroba fruit phenolic extract. Food Chemistry, 240, pp. 396-404, 2018. DOI: 10.1016/j.foodchem.2017.07.144
[16] Oliveira, D.A., Angonese, M., Ferreira, S.R.S. and Gomes, L., Food and bioproducts processing nanoencapsulation of passion fruit by-products extracts for enhanced antimicrobial activity. Food and Bioproducts Processing, 104, pp. 137-146, 2017. DOI: 10.1016/j.fbp.2017.05.009
[17] Wang, T., Ma, X., Lei, Y. and Luo, Y., Solid lipid nanoparticles coated with cross-linked polymeric double layer for oral delivery of curcumin. Colloids and Surfaces B: Biointerfaces, 148, pp. 1-11, 2016. DOI: 10.1016/j.colsurfb.2016.08.047
[18] Arunkumar, R., Prashanth, K.V.H., Manabe, Y., Hirata, T., Sugawara, T., Dharmesh, S.M. and Baskaran, V., Biodegradable poly (lactic-co-glycolic acid)-polyethylene glycol nanocapsules: an efficient carrier for improved solubility, bioavailability and anticancer property of lutein. Journal of Pharmaceutical Sciences, 104(6), pp. 2085-2093, 2015. DOI: 10.1002/jps.24436
[19] Liu, M., Yang, J., Ao, P. and Zhou, C., Preparation and characterization of chitosan hollow nanospheres for anticancer drug curcumin delivery. Materials Letters, 150, pp. 115-117, 2015. DOI: 10.1016/j.matlet.2015.03.013
[20] Natrajan, D., Srinivasan, S., Sundar, K. and Ravindran, A., Formulation of essential oil-loaded chitosan-alginate nanocapsules. Journal of Food and Drug Analysis, 23(3), pp. 560-568, 2015. DOI: 10.1016/j.jfda.2015.01.001
[21] Rigo, L.A., Da Silva, C.R., De Oliveira, S.M., Cabreira, T.N., De Bona Da Silva, C., Ferreira, J. and Beck, R.C.R., Nanoencapsulation of rice bran oil increases its protective effects against UVB radiation-induced skin injury in mice. European Journal of Pharmaceutics and Biopharmaceutics, 93, pp. 11-17, 2015. DOI: 10.1016/j.ejpb.2015.03.020
[22] Coradini, K., Lima, F.O., Oliveira, C.M., Chaves, P.S., Athayde, M.L., Carvalho, L.M. and Beck, R.C.R., Co-encapsulation of resveratrol and curcumin in lipid-core nanocapsules improves their in vitro antioxidant effects. European Journal of Pharmaceutics and Biopharmaceutics, 88(1), pp. 178-185, 2014. DOI: 10.1016/j.ejpb.2014.04.009
[23] Hill, L.E. and Gomes, C.L., Characterization of temperature and pH-responsive nanoparticles for the release of antimicrobials. Materials Research Express, 1, pp. 1-18, 2015. DOI: 10.1088/2053-1591/1/3/035405
[24] Silva, L.M., Hill, L.E., Figueiredo, E. and Gomes, C.L., Delivery of phytochemicals of tropical fruit by-products using poly (dl-lactide-co-glycolide) (PLGA) nanoparticles: synthesis, characterization, and antimicrobial activity. Food Chemistry, 165, pp. 362-370, 2014. DOI: 10.1016/j.foodchem.2014.05.118
[25] Hill, L.E., Taylor, T.M. and Gomes, C., Antimicrobial Efficacy of Poly (DL-lactide-co-glycolide) (PLGA) nanoparticles with entrapped cinnamon bark extract against listeria monocytogenes and salmonella typhimurium. Journal of Food Science, 78(4), pp. 1-49, 2013. DOI: 10.1111/1750-3841.12069
[26] Gomes, C., Moreira, R.G. and Castell-Perez, E., Poly (DL-lactide-co-glycolide) (PLGA) nanoparticles with entrapped trans-cinnamaldehyde and eugenol for antimicrobial delivery applications. Journal of Food Science, 76(2), pp. 16-24, 2011. DOI: 10.1111/j.1750-3841.2010.01985.x
[27] Kumari, A., Kumar, S., Pakade, Y.B., Singh, B. and Chandra, S., Development of biodegradable nanoparticles for delivery of quercetin. Colloids and Surfaces B: Biointerfaces, 80(2), pp. 184-192, 2010. DOI: 10.1016/j.colsurfb.2010.06.002
[28] Mukerjee, A. and Vishwanatha, J., Formulation, characterization and evaluation of curcumin-loaded PLGA nanoespheres for cancer therapy. Anticancer Research, [online]. 29, pp. 3867-3876, 2009. Available at: https://www.researchgate.net/publication/38027789
[29] Zigoneanu, I.G., Astete, C.E. and Sabliov, C.M., Nanoparticles with entrapped α -tocopherol: synthesis, characterization and controlled release. Nanotechnology, 19, pp. 1-8, 2008. DOI: 10.1088/0957-4484/19/10/105606
[30] Matich, D.J., Redes neuronales: conceptos básicos y aplicaciones. Historia, 55, 2001. Retrieved from ftp://decsai.ugr.es/pub/usuarios/castro/Material-Redes-Neuronales/Libros/matich-redesneuronales.pdf
[31] V.7, N.S. The neural network simulation environment. Getting started manual, V. 7, 2015.
[32] Hashad, R.A., Ishak, R.A.H., Fahmy, S., Mansour, S. and Geneidi, A.S., Chitosan-tripolyphosphate nanoparticles: optimization of formulation parameters for improving process yield at a novel pH using artificial neural networks. International Journal of Biological Macromolecules, 86, pp. 50-58, 2016. DOI: 10.1016/j.ijbiomac.2016.01.042
[33] Ochoa-Martínez, C.I. and Ayala-Aponte, A.A., Prediction of mass transfer kinetics during osmotic dehydration of apples using neural networks. LWT - Food Science and Technology, 40(4), pp. 638-645, 2007. DOI: 10.1016/j.lwt.2006.03.013
[34] Bourbon, A.I., Cerqueira, M.A. and Vicente, A.A., Encapsulation and controlled release of bioactive compounds in lactoferrin-glycomacropeptide nanohydrogels: curcumin and caffeine as model compounds. Journal of Food Engineering, 180, pp. 110-119, 2016. DOI: 10.1016/j.jfoodeng.2016.02.016
[35] Wang, J., Liao, X., Zheng, P., Xue, S. and Peng, R., Classification of chinese herbal medicine by laser induced breakdown spectroscopy with principal component analysis and Artificial Neural Network. Analytical Letters, 2719, pp. 1-24, 2017. DOI: 10.1080/00032719.2017.1340949
[36] Haykin, S., Neural networks a comprehensive foundation. 2nd Ed., Pearson Education, New Yersey, USA, 1999.

A.A. Ayala-Aponte, received his BSc. in Agricultural Engineering in 1993 from the Universidad del Valle, Cali, Colombia, and his PhD in Science and Food Technology in 2011 from the Universidad Politécnica de Valencia, Spain. He is a professor in the area of food technology and engineering, at the Universidad del Valle, Cali, Colombia. His research interests include: preservation and food processing.
ORCID: 0000-0003-0310-3577

C.I. Ochoa-Martínez, received her BSc. in Chemical Engineering in 1989, her MSc. in Chemical Engineering in 2001 and her PhD in Engineering in 2006. She has worked on projects in the food area since 2006 at the Universidad del Valle. She is currently a full time professor in the School of Food Engineering School, Universidad del Valle, Cali, Colombia. Her research interests include: modeling, simulation and drying process engineering and has several publications in scientific journals.
ORCID:0000-0002-2666-1726

L.A. Espinosa-Sandoval, received her BSc. in Food Engineering in 2012 from the Universidad del Valle, Cali, Colombia, and is currently a COLCIENCIAS fellow PhD Candidate in Engineering with an Emphasis in Food Engineering. Her research interests include: food processing, nanotechnology and mathematical modeling.
ORCID: 0000-0001-8813-2611